Astronomy & Astrophysics

Simultaneous multi-wavelength campaign on PKS 2005-489 in a high state

The H.E.S.S. Collaboration

A. Abramowski[1], F. Acero[2], F. Aharonian[3,4,5], A. G. Akhperjanian[6,5], G. Anton[7], A. Barnacka[8,9], U. Barres de Almeida[10,⋆], A. R. Bazer-Bachi[11], Y. Becherini[12,13], J. Becker[14], B. Behera[15], K. Bernlöhr[3,16], A. Bochow[3], C. Boisson[17], J. Bolmont[18], P. Bordas[19], V. Borrel[11], J. Brucker[7], F. Brun[13], P. Brun[9], T. Bulik[20], I. Büsching[21], S. Casanova[3], M. Cerruti[17], P. M. Chadwick[10], A. Charbonnier[18], R. C. G. Chaves[3], A. Cheesebrough[10], L.-M. Chounet[13], A. C. Clapson[3], G. Coignet[22], J. Conrad[23], M. Dalton[16], M. K. Daniel[10], I. D. Davids[24], B. Degrange[13], C. Deil[3], H. J. Dickinson[10,23], A. Djannati-Ataï[12], W. Domainko[3], L. O'C. Drury[4], F. Dubois[22], G. Dubus[25], J. Dyks[8], M. Dyrda[26], K. Egberts[27], P. Eger[7], P. Espigat[12], L. Fallon[4], C. Farnier[2], S. Fegan[13], F. Feinstein[2], M. V. Fernandes[1], A. Fiasson[22], G. Fontaine[13], A. Förster[3], M. Füßling[16], S. Gabici[4], Y. A. Gallant[2], H. Gast[3], L. Gérard[12], D. Gerbig[14], B. Giebels[13], J.F. Glicenstein[9], B. Glück[7], P. Goret[9], D. Göring[7], J. D. Hague[3], D. Hampf[1], M. Hauser[15], S. Heinz[7], G. Heinzelmann[1], G. Henri[25], G. Hermann[3], J. A. Hinton[28], A. Hoffmann[19], W. Hofmann[3], P. Hofverberg[3], D. Horns[1], A. Jacholkowska[18], O. C. de Jager[21], C. Jahn[7], I. Jung[7], M. A. Kastendieck[1], K. Katarzyński[30], U. Katz[7], S. Kaufmann[15], D. Keogh[10], M. Kerschhaggl[16], D. Khangulyan[3], B. Khélifi[13], D. Klochkov[19], W. Kluźniak[8], T. Kneiske[1], Nu. Komin[22], K. Kosack[9], R. Kossakowski[22], H. Laffon[13], G. Lamanna[22], J.-P. Lenain[17], D. Lennarz[3], T. Lohse[16], A. Lopatin[7], C.-C. Lu[3], V. Marandon[12], A. Marcowith[2], J. Masbou[22], D. Maurin[18], N. Maxted[31], T. J. L. McComb[10], M. C. Medina[9], J. Méhault[2], N. Nguyen[1], R. Moderski[8], E. Moulin[9], M. Naumann-Godo[9], M. de Naurois[13], D. Nedbal[32], D. Nekrassov[3], B. Nicholas[31], J. Niemiec[26], S. J. Nolan[10], S. Ohm[3], J.-F. Olive[11], E. de Oña Wilhelmi[3], B. Opitz[1], M. Ostrowski[29], M. Panter[3], M. Paz Arribas[16], G. Pedaletti[15], G. Pelletier[25], P.-O. Petrucci[25], S. Pita[12], G. Pühlhofer[19], M. Punch[12], A. Quirrenbach[15], M. Raue[1], S. M. Rayner[10], A. Reimer[27], O. Reimer[27], M. Renaud[2], R. de los Reyes[3], F. Rieger[3,33], J. Ripken[23], L. Rob[32], S. Rosier-Lees[22], G. Rowell[31], B. Rudak[8], C. B. Rulten[10], J. Ruppel[14], F. Ryde[34], V. Sahakian[6,5], A. Santangelo[19], R. Schlickeiser[14], F. M. Schöck[7], A. Schönwald[16], U. Schwanke[16], S. Schwarzburg[19], S. Schwemmer[15], A. Shalchi[14], M. Sikora[8], J. L. Skilton[35], H. Sol[17], G. Spengler[16], Ł. Stawarz[29], R. Steenkamp[24], C. Stegmann[7], F. Stinzing[7], I. Sushch[16], A. Szostek[29,25], P. H. Tam[15], J.-P. Tavernet[18], R. Terrier[12], O. Tibolla[3], M. Tluczykont[1], K. Valerius[7], C. van Eldik[3], G. Vasileiadis[2], C. Venter[21], J. P. Vialle[22], A. Viana[9], P. Vincent[18], M. Vivier[9], H. J. Völk[3], F. Volpe[3], S. Vorobiov[2], M. Vorster[21], S. J. Wagner[15], M. Ward[10], A. Wierzcholska[29], A. Zajczyk[20], A. A. Zdziarski[8], A. Zech[17], H.-S. Zechlin[1]

The *Fermi* LAT Collaboration

A. A. Abdo[36], M. Ackermann[37], M. Ajello[37], L. Baldini[38], J. Ballet[9], G. Barbiellini[39,40], D. Bastieri[41,42], K. Bechtol[37], R. Bellazzini[38], B. Berenji[37], R. D. Blandford[37], E. Bonamente[43,44], A. W. Borgland[37], J. Bregeon[38], A. Brez[38], M. Brigida[45,46], P. Bruel[13], R. Buehler[37], S. Buson[41,42], G. A. Caliandro[47], R. A. Cameron[37], A. Cannon[48,49], P. A. Caraveo[50], S. Carrigan[42], J. M. Casandjian[9], E. Cavazzuti[51], C. Cecchi[43,44], Ö. Çelik[48,52,53], A. Chekhtman[54,55], C. C. Cheung[36], J. Chiang[37], S. Ciprini[44], R. Claus[37], J. Cohen-Tanugi[23], S. Cutini[51], C. D. Dermer[54], F. de Palma[45,46], E. do Couto e Silva[37], P. S. Drell[37], R. Dubois[37], D. Dumora[56], L. Escande[56,57], C. Favuzzi[45,46], E. C. Ferrara[48], W. B. Focke[37], P. Fortin[13], M. Frailis[58,59], Y. Fukazawa[60], P. Fusco[45,46], F. Gargano[46], D. Gasparrini[51], N. Gehrels[48], S. Germani[43,44], N. Giglietto[45,46], P. Giommi[51], F. Giordano[45,46], M. Giroletti[61], T. Glanzman[37], G. Godfrey[37], I. A. Grenier[9], J. E. Grove[54], S. Guiriec[62], D. Hadasch[47], E. Hays[48], D. Horan[13], R. E. Hughes[63], G. Jóhannesson[64], A. S. Johnson[37], W. N. Johnson[54], T. Kamae[37], H. Katagiri[60], J. Kataoka[65], J. Knödlseder[66], M. Kuss[38], J. Lande[37], L. Latronico[38], S.-H. Lee[37], F. Longo[39,40], F. Loparco[45,46], B. Lott[56], M. N. Lovellette[54], P. Lubrano[43,44], G. M. Madejski[37], A. Makeev[54,55], M. N. Mazziotta[46], W. McConville[48,67], J. E. McEnery[48,67], P. F. Michelson[37], T. Mizuno[60], C. Monte[45,46], M. E. Monzani[37], A. Morselli[68], I. V. Moskalenko[37], S. Murgia[37], T. Nakamori[65], S. Nishino[60], P. L. Nolan[37], J. P. Norris[69], E. Nuss[23], T. Ohsugi[70], A. Okumura[71], N. Omodei[37], E. Orlando[72], J. F. Ormes[69], M. Ozaki[71], D. Paneque[37], J. H. Panetta[37], D. Parent[73], V. Pelassa[23], M. Pepe[43,44], M. Pesce-Rollins[38], F. Piron[23], T. A. Porter[37], S. Rainò[45,46], R. Rando[41,42], M. Razzano[38], H. F.-W. Sadrozinski[74], D. Sanchez[13], A. Sander[63], C. Sgrò[38], E. J. Siskind[75], P. D. Smith[63], G. Spandre[38], P. Spinelli[45,46], M. S. Strickman[54], D. J. Suson[76], H. Takahashi[70], T. Takahashi[71], T. Tanaka[37], J. B. Thayer[37], J. G. Thayer[37], D. J. Thompson[48], L. Tibaldo[41,42,9,77], D. F. Torres[47,78], G. Tosti[43,44], A. Tramacere[37,79,80], E. Troja[48,81], T. Uehara[60], T. L. Usher[37], J. Vandenbroucke[37], G. Vianello[37,86], N. Vilchez[66], V. Vitale[68,82], A. P. Waite[37], P. Wang[37], B. L. Winer[63], K. S. Wood[54], Z. Yang[24,25], T. Ylinen[83,84,25], and M. Ziegler[74]

(Affiliations can be found after the references)

ABSTRACT

The high-frequency peaked BL Lac object PKS 2005-489 was the target of a multi-wavelength campaign with simultaneous observations in the TeV γ-ray (H.E.S.S.), GeV γ-ray (*Fermi*/LAT), X-ray (RXTE, Swift), UV (Swift) and optical (ATOM, Swift) bands. This campaign was carried out during a high flux state in the synchrotron regime. The flux in the optical and X-ray bands reached the level of the historical maxima. The hard GeV spectrum observed with *Fermi*/LAT connects well to the very high energy (VHE, $E > 100$ GeV) spectrum measured with H.E.S.S.

with a peak energy between ~5 and 500 GeV. Compared to observations with contemporaneous coverage in the VHE and X-ray bands in 2004, the X-ray flux was ~50 times higher during the 2009 campaign while the TeV γ-ray flux shows marginal variation over the years. The spectral energy distribution during this multi-wavelength campaign was fit by a one zone synchrotron self-Compton model with a well determined cutoff in X-rays. The parameters of a one zone SSC model are inconsistent with variability time scales. The variability behaviour over years with the large changes in synchrotron emission and small changes in the inverse Compton emission does not warrant an interpretation within a one-zone SSC model despite an apparently satisfying fit to the broadband data in 2009.

Key words. galaxies: active – BL Lacertae objects: individual: PKS 2005-489

1. Introduction

PKS 2005-489 is one of the brightest high-frequency peaked BL Lac objects (HBL) in the southern hemisphere. It is located at $\alpha_{J2000} = 20^h09^m25.39^s$, $\delta_{J2000} = -48°49'53.7''$ (Johnston et al. 1995) and has a redshift of $z = 0.071$ (Falomo et al. 1987).

HBL are characterized by two peaks in their spectral energy distribution (SED) which are located in the UV-X-ray and the GeV−TeV band, respectively. These are commonly explained by leptonic models (e.g. Marscher & Gear 1985) as synchrotron and inverse Compton (IC) emission from a population of relativistic electrons upscattering their self-produced synchrotron photons (Synchrotron Self Compton models (SSC)). Also alternative models based on hadronic interactions exist, e.g. Mannheim (1993).

PKS 2005-489 was detected through the Parkes 2.7 GHz survey (Wall et al. 1975) and is part of the 1 Jy catalog (Kühr et al. 1981) of the brightest extragalactic radio sources.

It has been observed during several years by different X-ray satellites and showed very large flux variations in combination with distinct spectral changes. In October−November 1998, a large X-ray flare was detected and monitored with RXTE (Perlman et al. 1999). Shortly before this flare occured, *BeppoSAX* observations were conducted which revealed a curved X-ray spectrum from 0.1 to 200 keV with photon indices of $\Gamma_1 = 2$, $\Gamma_2 = 2.2$ and a break around 2 keV (Tagliaferri et al. 2001).

The first evidence for γ-ray emission was marginally detected (4.3σ) with the EGRET instrument revealing a flux of $F(>100\,\text{MeV}) = (1.3 \pm 0.5) \times 10^{-7}\,\text{cm}^{-2}\,\text{s}^{-1}$ (Lin et al. 1999; Nandikotkur et al. 2007). This made PKS 2005-489 one of the few HBL detected by EGRET. Very high energy (VHE, $E > 100$ GeV) γ-rays from PKS 2005-489 were first detected by the Cherenkov telescope array H.E.S.S. (High Energy Stereoscopic System) (Aharonian et al. 2005). Multi-year studies of the TeV emission by H.E.S.S. together with several multi-wavelength observations are described by the H.E.S.S. Collaboration (2010). The VHE γ-ray spectra can be described by power laws with photon indices varying between 2.9 and 3.7 and hence they are amongst the softest spectra of all VHE γ-ray active galactic nuclei (AGN).

Together with the *Fermi* Gamma-ray Space Telescope (in operation since June 2008) it is possible to determine the inverse Compton emission peak of PKS 2005-489. Together with simultaneous broadband observations, the underlying emission processes can be studied in more detail. In this paper the results of such a broadband simultaneous multi-wavelength campaign on PKS 2005-489 conducted in 2009 are presented.

2. Multi-wavelength observations and data analysis

A multi-wavelength campaign on PKS 2005-489 was conducted from May 22 to July 2, 2009 with observations by the Cherenkov telescope array H.E.S.S. (High Energy Stereoscopic System),
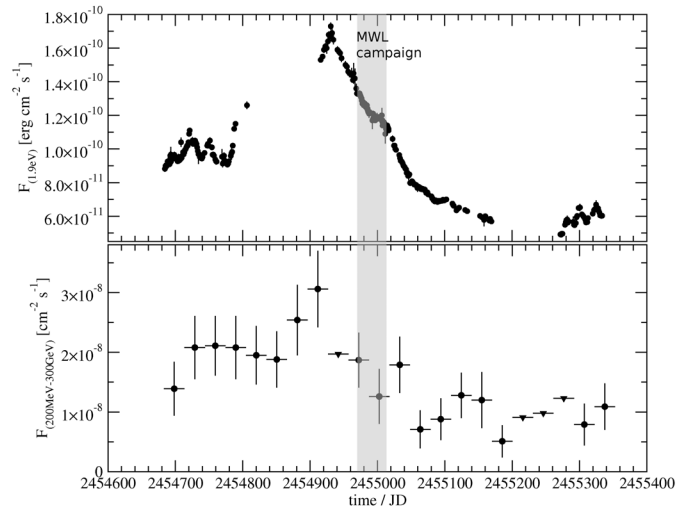
Fig. 1. Long term lightcurves of PKS 2005-489 over 22 months of the optical emission (*upper panel*) by ATOM and the HE γ-ray emission (*lower panel*) by *Fermi*/LAT. The HE γ-ray lightcurve is binned with 30 days intervals. The triangles represent upper limits. The major gaps in the optical lightcurve are due to solar conjunction. The grey band indicates the time of the multi-wavelength campaign from May 22 to July 2, 2009.

the X-ray satellites RXTE (Rossi X-ray Timing Explorer) and Swift and the optical 75-cm telescope ATOM (Automatic Telescope for Optical Monitoring for H.E.S.S.). The LAT (Large Area Telescope) instrument onboard the *Fermi* Gamma-ray Space Telescope scans the whole sky within approximately 3 h and hence PKS 2005-489 was regularly monitored during this campaign such that simultaneous information about the brightness and the spectrum of the high energy (HE, 100 MeV $< E <$ 100 GeV) γ-ray emission could be obtained. Hence, for the first time, simultaneous observations have been taken on PKS 2005-489 in the VHE, HE γ-ray, X-ray, UV and optical bands, that can be used for variability and spectral studies. The simultaneous monitoring by Fermi in the GeV and by ATOM in the optical band over a time of 22 months allows the study of the long term behaviour of PKS 2005-489. The time of the multi-wavelength campaign is marked in the long term light curve shown in Fig. 1.

2.1. Very high energy γ-ray data from H.E.S.S.

The H.E.S.S. experiment consists of four imaging atmospheric Cherenkov telescopes, located in the Khomas Highland, Namibia (23°16′18″ South, 16°30′00″ East), at an elevation of 1800 m (Aharonian et al. 2006a). The observations on PKS 2005-489 have been taken with a mean zenith angle of 27° from May 22 to July 2, 2009 with a break around full moon since H.E.S.S. does not observe during moontime. The data have been calibrated as described in Aharonian et al. (2004) and analyzed using the *standard cuts* resulting in an energy

threshold of ≈400 GeV and following the method described in Aharonian et al. (2006a). After the standard quality selection 13 h of live time remain. A total of N_{ON} = 953 on-source and N_{OFF} = 5513 off-source events with an on-off normalization factor of α = 0.0932 were measured. An excess of $N_\gamma = N_{ON} - \alpha N_{OFF}$ = 439 γ-rays, corresponding to a significance of 16σ (following the method of Li & Ma 1983), results for PKS 2005-489 within the whole observing period. The *reflected-region* method (Aharonian et al. 2006a) was used for background subtraction of the spectrum. The same data have been analyzed using a different calibration, resulting in compatible results.

2.2. High energy γ-ray data from Fermi/LAT

The *Fermi* LAT is a pair-conversion γ-ray detector sensitive to photons in the energy range from below 20 MeV to more than 300 GeV (Atwood et al. 2009). Launched by NASA on June 11, 2008, the LAT began nominal science operations on August 4, 2008. The LAT observations presented here comprise all the data taken between August 4, 2008 and June 4, 2010 (22 months), which fully covers the H.E.S.S. observations taken from May 22 to July 2, 2009. The LAT Science Tools[1] version v9r15 were utilized with the post-launch instrument response functions (IRF) P6_V3_DIFFUSE. Events with high probability of being photons, those from the *diffuse* class, and with zenith angles <105° were selected. Time intervals during which the rocking angle (i.e. the angle *Fermi* points north or south of the zenith on alternate orbits during sky survey operations) was larger than 52° were excluded to avoid contamination from the Earth's limb. A cut at 200 MeV was used to avoid the larger systematic uncertainties in the analysis at lower energies. Events with energy between 200 MeV and 300 GeV, and within a 10° region of interest (ROI) centered on the coordinates of PKS 2005-489 were analyzed with an unbinned maximum likelihood method (Cash 1979; Mattox et al. 1996). Some sources from the 1FGL catalog (Abdo et al. 2010) were located outside the ROI but close and bright enough to have a significant impact on the analysis. These sources have been taken into account in the analysis. The background emission was modeled using standard Galactic and isotropic diffuse emission models[2]. The 1FGL catalog (Abdo et al. 2010) and a Test Statistic (TS, where $TS = -2\Delta \log(\text{likelihood})$ between models with and without the source) map of the region around PKS 2005-489 were used to identify all the point sources within the ROI. The point sources and PKS 2005-489 were modeled using a power law of the form $F(E) = N_0(E/E_0)^{-\Gamma}$.

The likelihood analysis reveals a point source with a high statistical significance ($\sigma \propto \sqrt{TS} > 20$). The best-fit position of this point source was calculated with gtfindsrc (α_{J2000} = 20^{h}09^{m}25.0^s, δ_{J2000} = $-48°49'44.4''$) and has a 95% containment radius of 1.5′, consistent with the coordinates of PKS 2005-489. The highest energy photon associated with the source has an energy of ~180 GeV and was detected on March 10, 2009 (i.e. before the start of the H.E.S.S. observations). The highest energy photon detected by *Fermi*/LAT during the H.E.S.S. multi-wavelength campaign has an energy of ~50 GeV and was detected on June 1, 2009.

2.3. X-ray data from RXTE and Swift/XRT

X-ray observations with the Proportional Counter Array (PCA) detector onboard RXTE (Bradt et al. 1993) were obtained in the energy range 2−60 keV from May 22 to June 3 with exposures of 2−4 ks per pointing, strictly simultaneous with good quality H.E.S.S. observations in 6 nights. Due to the high state of PKS 2005-489 during this campaign, additional Target of Opportunity (ToO) observations have been taken with the X-ray satellites Swift and RXTE. The XRT detector (Burrows et al. 2005) onboard Swift observed in photon-counting (PC) and windowed-timing (WT) mode in the energy range 0.2−10 keV on June 1 and June 24 with ~3 ks each. The RXTE ToO observations were performed from June 30 to July 3, 2009.

For the data analysis of the data obtained with RXTE and Swift, the software package HEASoft[3] was used.

Only RXTE/PCA data of PCU2 and the top layer 1 were taken into account to obtain the best signal-to-noise ratio. The data were filtered to account for the influence of the South Atlantic Anomaly, tracking offsets, and electron contamination using the standard criteria recommended by the RXTE Guest Observer Facility (GOF). For the count rate of ~9 cts/s for this observations, the faint background model provided by the RXTE GOF for count rates <40 cts/s was used to generate the background spectrum with pcabackest and the response matrices were created with pcarsp.

The second instrument onboard RXTE, the HEXTE (High Energy X-ray Timing Experiment) is measuring in the energy range 15 to 250 keV. For PKS 2005-489, a signal was detected only in the sum of all observations during the campaign. The fit of a power law to the combined PCA and HEXTE spectrum gives the same result as for the PCA spectrum alone. The combined fit is dominated by the more sensitive PCA detector with a better signal to noise ratio. Hence, the HEXTE spectrum is not discussed further.

For the Swift spectral analysis, XRT exposure maps were generated with xrtpipeline to account for some bad CCD columns that are masked out on-board. The masked hot columns appeared when the XRT CCD was hit by a micrometeoroid. Spectra of the Swift data in PC-mode have been extracted with xselect from an annulus region with an outer radius of 0.8′ at the position of PKS 2005-489, which contains 90% of the PSF at 1.5 keV and an inner radius of ~0.1′ to avoid pileup. An appropriate background was extracted from a circular region with radius of 3′ nearby the source. For the WT-mode, appropriate boxes (~1.6′ × 0.3′) covering the region with source photons and a background region with similar size were used to extract the spectra. The auxiliary response files were created with xrtmkarf and the response matrices were taken from the Swift package of the calibration database caldb 4.1.3[4].

A power law of the form $F(E) = N_0(E/E_0)^{-\Gamma}$ was used to fit the X-ray spectra of each pointing obtained by RXTE in the energy range 3−20 keV resulting in consistent parameters and an average photon index of Γ = 2.46 ± 0.03. During this campaign, no significant change in spectral shape was found. The detailed spectral analysis and results are discussed in Sect. 4.2.
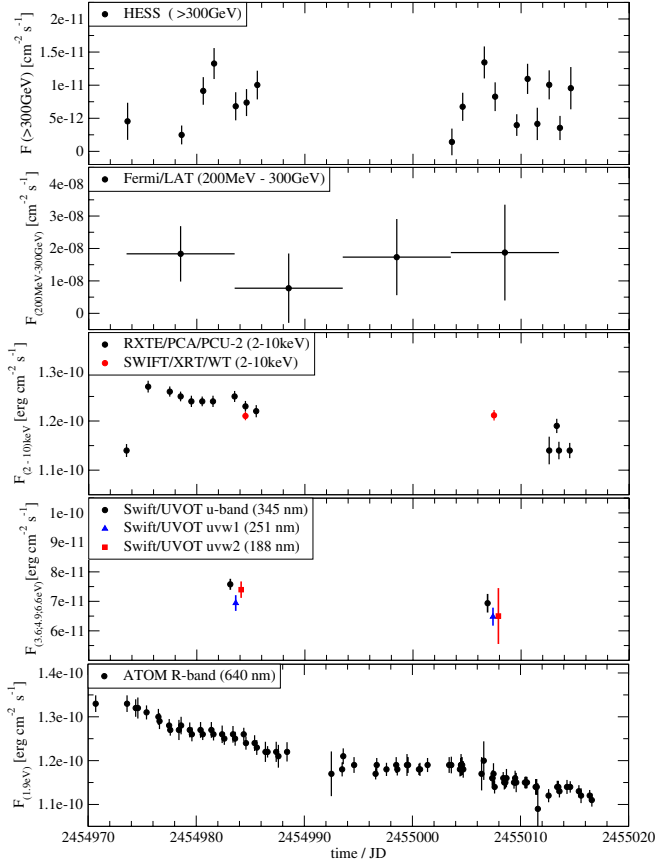
Fig. 2. Lightcurves of PKS 2005-489 during the multi-wavelength campaign from May 22 to July 2, 2009 with observations by the Cherenkov telescope array H.E.S.S., the γ-ray space telescope *Fermi*, the X-ray satellites RXTE and Swift and the 75-cm optical telescope ATOM. For a better display, the u and *uvw*2 band data by Swift are shifted by ±0.5 days. For the H.E.S.S., RXTE and Swift lightcurves a nightly binning was used and the *Fermi*/LAT lightcurve is shown in a 10-day binning.

2.4. UV data from Swift/UVOT

The UVOT instrument (Roming et al. 2005) onboard Swift measures the UV emission in the bands u (345 nm), *uvw*1 (251 nm) and *uvw*2 (188 nm) simultaneous to the X-ray telescope with an exposure of ~1 ks each. The instrumental magnitudes and the corresponding flux (conversion factors see Poole et al. 2008) are calculated with `uvotmaghist` taking into account all photons from a circular region with radius 5″ (standard aperture for all filters). An appropriate background was determined from a circular region with radius 40″ near the source region without contamination of sources.

The measured UV fluxes have been corrected for dust absorption using $E(B - V) = 0.056$ mag (Schlegel et al. 1998) and the $A_\lambda / E(B - V)$ ratios given in Giommi et al. (2006) resulting in a correction of 35%, 29%, 24% for *uvw*2, *uvw*1 and *u*-band, respectively. The contribution of the host galaxy to the measured flux is small compared to the correction for extinction and was not taken into account.

2.5. Optical data from ATOM

The 75-cm telescope ATOM (Hauser et al. 2004), located at the H.E.S.S. site in Namibia, monitored the flux in the 4 different filters: *B* (440 nm), *V* (550 nm), *R* (640 nm) and *I* (790 nm)

according to Bessell (1990). The obtained data have been analyzed using an aperture of 4″ radius and differential photometry with three nearby reference stars from the USNO catalog (Monet & et al. 1998) to determine the apparent magnitudes.

The host galaxy of PKS 2005-489 is a giant elliptical galaxy with a brightness of 14.5 mag (*R*-band) and a half-light radius of 5.6″ (Scarpa et al. 2000). In order to correct for the host galaxy light, a de Vaucouleur profile of the galaxy was assumed and rescaled to the aperture used in the ATOM photometry. To calculate the influence of the host galaxy in the *B*, *V* and *I* filter, the spectral template for a nearby elliptical galaxy by Fukugita et al. (1995) has been used. The galactic extinction calculated for the ATOM filters is negligible compared to the host galaxy contribution.

3. Temporal analysis

The multiwavelength observations taken from May 22 to July 2 2009 were used to search for variability during the phase of high flux. The lightcurves of this campaign are shown in Fig. 2.

3.1. Variation in different energy bands

Very high energy emission has been detected with a mean flux of $F(>300 \, \text{GeV}) = (6.7 \pm 0.5) \times 10^{-12} \, \text{cm}^{-2} \, \text{s}^{-1}$ for the time of the campaign. The measured flux level is ~2 times brighter than during the detection of this source in 2004 by H.E.S.S. (H.E.S.S. Collaboration 2010). While no significant long-term trend is detected during the six weeks of observations, a constant flux provides a poor fit with a χ^2/d.o.f. = 50/16 and a probability of $p < 0.1\%$. The nightly binned flux shows evidence for variability of about a factor of 2. The low signal to noise ratio does not allow a precise determination of time scales.

PKS 2005-489 was detected by the LAT during the period corresponding to the H.E.S.S. multi-wavelength campaign (TS = 69). Due to the rather faint HE emission, the binning of the light curve for the time period of this campaign was chosen to be 10 days. Within the limited statistics, no variations were detected on these short time scales.

The high X-ray flux of PKS 2005-489 is comparable to the historical maximum of 1998 (Perlman et al. 1999; Tagliaferri et al. 2001). The X-ray flux increased by 10% within the first 2 days of the campaign and decreased until the end of the campaign back to the initial flux level.

The nightly binned *u*, *uvw*1 and *uvw*2-band observations with the Swift/UVOT detector do not show any variation.

The high optical flux measured by ATOM in all 4 filters decreases monotonically by ~20% during this campaign. The colors remained constant with averages of $B - R = 1.36$ mag, $V - R = 0.78$ mag and $R - I = 0.08$ mag.

The long term lightcurves of the optical and HE γ-ray emission of PKS 2005-489 over 22 months is shown in Fig. 1. The maximum in the optical band is clearly identified at 2 454 930.7 JD. The *Fermi*/LAT light curve displays a variation in the monthly binning with an amplitude similar to the optical variation. A fit with a constant flux results in a poor description with a χ^2/d.o.f. = 41 / 17 and a probability of $p < 1\%$. The decrease in the second half of the light curve has a significance of ~4.5σ. In the monthly binning of the light curve, the identification of the maximum is uncertain by ~30 day. Considering this, it is marginally consistent with the maximum of the synchrotron emission.
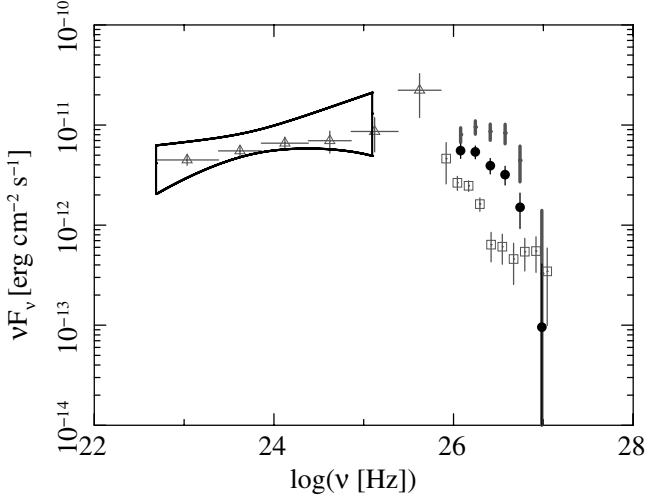
Fig. 3. The γ-ray energy spectra of PKS 2005-489 covering the inverse Compton peak of the spectral energy distribution. In black, the γ-ray spectra (*Fermi*/LAT as butterfly and H.E.S.S. as circles) of this simultaneous multi-wavelength campaign are denoted. In grey open symbols, historical and time-averaged data are shown: triangles represent the *Fermi*/LAT spectrum from 22 months of observations and the squares show the integrated H.E.S.S. spectrum extracted from observations from 2004 to 2007 (H.E.S.S. Collaboration 2010). Dark grey bars denote the VHE γ-ray spectrum of 2009, corrected for the absorption by the extragalactic background light. The size of the bar reflects the highest and smallest correction, including the statistical and systematic uncertainties, using the models by Aharonian et al. (2006b) and Franceschini et al. (2008).

3.2. Correlations

The highest flux measured in the X-ray band seems to follow the high flux measured in the optical before the beginning of this campaign. In both wavebands a slow decrease could be measured over the time period of this campaign, where the optical flux decreases by ~20% and the X-ray flux by ~10%. The correlation coefficient (also known as Pearson's correlation) of the optical *R*-band from ATOM and the X-ray flux from RXTE is 0.7 for the full time range. Considering only the decaying part of the X-ray lightcurve, this factor increases to 0.96. A change of similar amplitude could not be detected with the *Fermi*/LAT due to the large uncertainties.

Interestingly, the variation in the VHE flux, e.g. the increase in flux between 2 454 978 and 2 454 982 JD is not seen in the simultaneous X-ray and optical observations which do not vary significantly during this period.

4. Spectral energy distribution

For the first time, simultaneous observations from optical to VHE have been obtained on PKS 2005-489, providing a very good coverage of the emission peaks seen in the spectral energy distribution (SED) (see Figs. 3 and 4).

4.1. Spectral data in the γ-ray range

The measured very high energy spectrum by H.E.S.S. (see Fig. 3) during the period of this campaign, can be described by a power law ($N(E) = N_0 \times (E/E_0)^{-\Gamma}$) with a normalization of $N_0 = (2.1 \pm 0.2_{stat} \pm 0.4_{sys}) \times 10^{-12}$ cm^{-2} s^{-1} TeV^{-1} at $E_0 = 1$ TeV and a spectral index of $\Gamma = 3.0 \pm 0.1_{stat} \pm 0.2_{sys}$ (χ^2/d.o.f. = 13/4). The subscripts refer to statistical and systematic uncertainties.
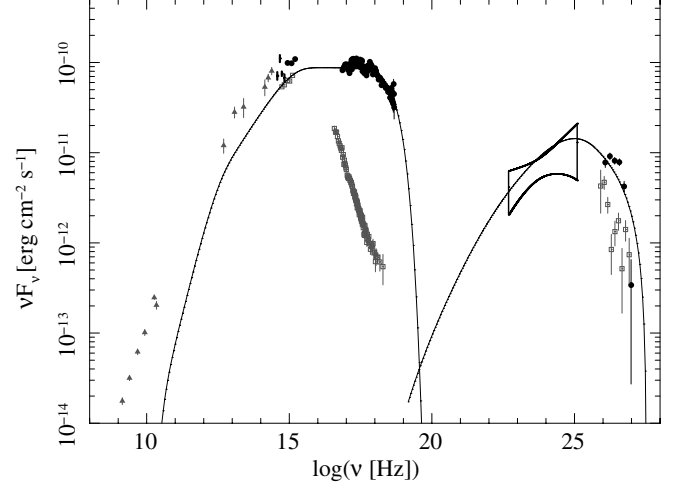
Fig. 4. Spectral energy distribution of PKS2005-489 during this multi-wavelength campaign with simultaneous observations by H.E.S.S., *Fermi*/LAT, RXTE, Swift and ATOM (black symbols) using the time range shown in Fig. 1. The spectra shown here are corrected for Galactic extinction, N_H absorption, and EBL absorption. The size of the symbols for the optical data represent the flux range measured. The de-absorbed X-ray and TeV spectra of PKS 2005-489 in 2004 (H.E.S.S. Collaboration 2010), as well as historical IR and radio observations are shown in grey. The black curves represent a one zone SSC model as described in the text.

A power law with an exponential cutoff with a normalization of $N_0 = (1.1 \pm 0.6_{stat} \pm 0.2_{sys}) \times 10^{-11}$ cm^{-2} s^{-1} TeV^{-1} at $E_0 = 0.5$ TeV, a photon index of $\Gamma = 1.3 \pm 0.6_{stat} \pm 0.2_{sys}$ and a cutoff at $E_{cutoff} = 1.3 \pm 0.5_{stat}$ TeV is a much better description than the simple power law.

This VHE spectrum has been corrected for the absorption by the extragalactic background light (EBL) using the models by Aharonian et al. (2006b) and Franceschini et al. (2008). In Fig. 3 the minima and maxima of this correction are shown to illustrate the uncertainties of this correction. Since the measurement errors cover the uncertainties using different EBL models, only one model has been chosen for the overall SED shown in Fig. 4.

The time averaged very high energy spectrum from 2004–2007 (shown in Fig. 3) can be described by a power law with a spectral index of $\Gamma = 3.2 \pm 0.16_{stat} \pm 0.1_{sys}$, consistent with the one obtained during this campaign but does not show significant curvature (H.E.S.S. Collaboration 2010).

During this campaign PKS 2005-489 shows a marginally harder TeV spectrum than during its TeV detection in 2004 (H.E.S.S. Collaboration 2010) when the softest spectrum of a TeV blazar with spectral index of $\Gamma = 3.7 \pm 0.4_{stat} \pm 0.1_{sys}$ was measured. This spectrum, obtained in 2004, with contemporaneous X-ray, UV and optical observations is shown in Fig. 4 for comparison. Most noticeable in the comparison is the indication of a cutoff in the VHE spectrum of this campaign and the different normalizations which suggest a change of the inverse Compton peak to higher energies in 2009. The VHE spectrum resulting from this multi-wavelength campaign and from 2004 have been corrected for the absorption by the EBL using the model by Franceschini et al. (2008) and are shown in Fig. 4.

The averaged *Fermi*/LAT photon spectrum during the time of this campaign is fitted by a power law for which the normalization constant N_0 is $(0.62 \pm 0.04_{stat} \pm 0.02_{sys}) \times 10^{-12}$ cm^{-2} s^{-1} MeV^{-1}, the spectral index Γ is $1.79 \pm 0.05_{stat} \pm 0.07_{sys}$, and $E_0 = 2385$ MeV is the energy at which the

correlation between the fitted values of the normalization constant and the spectral index is minimized. Changing the model of the spectrum to a log-parabola does not improve the quality of the spectral fit significantly. Spectral points were obtained by dividing the data into six equal logarithmically-spaced energy bands. A separate likelihood analysis was run over each band. For all sources in the model of the region, the index was frozen to the time-independent best-fit value, and the flux was left free to vary.

PKS 2005-489 is too faint in the HE band to obtain spectral points for the epoch of the H.E.S.S. multi-wavelength campaign. A 1-sigma error contour (butterfly) was calculated using the covariance matrix produced during the `gtlike` likelihood fit (Abdo et al. 2009). The full energy range (200 MeV–300 GeV) was used for the fit but the butterfly was extended to only 50 GeV to include the highest energy photon detected during the multi-wavelength campaign.

The HE spectral points obtained for the 22-month period and the butterfly calculated for the H.E.S.S. multi-wavelength campaign are shown in Fig. 3.

4.2. Spectral data in the synchrotron range

PKS 2005-489 was in a very high X-ray state during this campaign with a maximum flux comparable to the historical maximum of 1998. The spectrum during the 2009 campaign was determined from the sum of all RXTE and Swift observations. In the energy range of 0.3–20 keV it can be described by a broken power law with $\Gamma_1 = 2.02 \pm 0.01$, $\Gamma_2 = 2.46 \pm 0.01$, break energy at 3.2 ± 0.2 keV and a normalisation of $N_0 = (5.80 \pm 0.06) \times 10^{-2}$ cm^{-2} s^{-1} keV^{-1} at $E_0 = 1$ keV (χ^2/d.o.f. $= 582/373$), using the Galactic absorption of 3.94×10^{20} cm^{-2} (LAB Survey, Kalberla et al. 2005) as a fixed parameter. This spectrum by RXTE and Swift corrected for the Galactic absorption is shown in Fig. 4. The integrated flux between 2 and 10 keV is $F_{(2-10\,\text{keV})} = (1.23 \pm 0.01) \times 10^{-10}$ erg cm^{-2} s^{-1} which is a factor of ~100 higher than the integrated flux of the *XMM-Newton* observation in 2004 (H.E.S.S. Collaboration 2010) while the monochromatic flux at 2 keV is ~50 times higher than in 2004.

The two X-ray instruments had different sampling patterns. Since variability was detected during the entire campaign, a joint spectral fit was obtained on June 1, 2009. The derived broken power law model was fit, resulting in $\Gamma_1 = 2.04 \pm 0.02$, $\Gamma_2 = 2.50 \pm 0.07$, break energy at 3.8 ± 0.4 keV and a normalisation of $N_0 = (5.72 \pm 0.07) \times 10^{-2}$ cm^{-2} s^{-1} keV^{-1} at $E_0 = 1$ keV (χ^2/d.o.f. $= 493/302$), which is consistent to the fit of the summed spectra. The integrated flux is $F_{(2-10\,\text{keV})} = (1.23 \pm 0.01) \times 10^{-10}$ erg cm^{-2} s^{-1}.

In Fig. 4 a dip at the low energy end of the X-ray spectrum can be seen. As discussed by Godet et al. (2009), the most likely explanation for this feature is a detector effect.

The spectrum obtained during the historical maximum on November 10, 1998 is described by a power law of $\Gamma = 2.35 \pm 0.02$ with a flux of $F_{(2-10\,\text{keV})} = 3.3 \times 10^{-10}$ erg cm^{-2} s^{-1}(Perlman et al. 1999). The *BeppoSAX* spectrum, obtained eight days before on November 1–2, could be fitted with a broken power law with $\Gamma_1 = 2.02 \pm 0.04$, $\Gamma_2 = 2.21 \pm 0.02$, $E_{\text{break}} = 1.9 \pm 0.4$ keV ($F_{(2-10\,\text{keV})} = 1.8 \times 10^{-10}$ erg cm^{-2} s^{-1}) using a fixed Galactic absorption of 4.2×10^{20} cm^{-2} (Tagliaferri et al. 2001). Compared to the spectral shape of these observations, the high energy photon index of the broken power law detected in the 2009 campaign is higher ($\Delta\Gamma \approx 0.3$) and the peak is at a slightly higher energy.

Since the spectrum at the time of the historical maximum was obtained with RXTE in the energy range 2–10 keV, a spectral break <2–3 keV cannot be ruled out.

IR observations have been obtained between September 28 and October 1, 1998 with the 2.5 m Telescope at the Las Campanas Observatory using the NIR camera with J_s (1.24 μm), H (1.65 μm), K_s (2.16 μm) (Cheung et al. 2003). The observed fluxes were corrected for the influence of the host galaxy in these bands and are shown in Fig. 4. PKS 2005-489 is also detected in the frequencies 12 μm, 25 μm, 60 μm with the Infrared Astronomical Satellite (IRAS) as mentioned in the IRAS faint source catalog v2[5] (Moshir 1990).

Radio observations of PKS 2000-489 with the Australian Telescope Compact Array (ATCA) at the frequencies 8.6, 4.8, 2.5, 1.4 GHz have been done from October 1996 to February 2000 (Tingay et al. 2003). It was also observed with ATCA in the frequencies 18.5 GHz and 22 GHz in March 2002 (Ricci et al. 2006) during measurements of all sources of the 5 GHz 1 Jy-catalog (Kühr et al. 1981).

PKS 2005-489 is known to be variable in the synchrotron range, therefore the historical IR and radio observations are not taken into account for the SED modelling.

4.3. SED model

The multi-wavelength data obtained during this campaign cover well the two emission peaks in the spectral energy distribution (see Fig. 4) allowing the simultaneous determination of the peak energies and fluxes of the two spectral components.

A one zone SSC model using the code by Krawczynski et al. (2004) has been applied to create a model that can describe the simultaneously observed multi-wavelength SED of this campaign.

The specific spectral shape (broken power law) in the X-ray band is a strong restriction for the cutoff in the synchrotron emission and therefore limits the maximum energy of the electron distribution. The optical, UV and X-ray spectra describing the synchrotron emission restrict the parameters of the electron distribution. This distribution can be described by a broken power law with indices $n_1 = 2$ and $n_2 = 3$, as well as the minimum $E_{\text{min}} = 7.9 \times 10^8$ eV ($\gamma = 1.5 \times 10^3$), break $E_b = 2 \times 10^{10}$ eV ($\gamma = 3.9 \times 10^4$) and maximum energy $E_{\text{max}} = 1 \times 10^{12}$ eV ($\gamma = 2 \times 10^6$). The high energy power law photon index has been chosen such that the flat shape of the SED in the UV to X-ray range is reproduced. The difference in indices of the broken power law follows the standard break due to cooling ($n_2 - n_1 = 1$).

In order to explain the measured inverse Compton emission in view of the large separation to the synchrotron peak, the remaining parameters describing the emission volume were chosen as 15 for the Doppler factor, $R = 4 \times 10^{17}$ cm for the radius and 0.02 G for the magnetic field. The Doppler factor of 15 was found to be the smallest possible to reproduce the measured shape. The resulting SSC model can well describe the measured broadband SED. However, this leads to R/δ by a factor of ≈ 3 larger (corresponding to a variability time scale of approx. 9 days) than the value determined from the variability time scale of a few days detected for the source. In order to correct this, a Doppler factor of around 50 would be needed, but this would lead to a lower synchrotron peak frequency and the cutoff in the synchrotron emission detected in the X-ray band can not

---

[5] `http://vizier.cfa.harvard.edu/viz-bin/Cat?II/156A`

be described after adjusting the parameters to reduce the large fluxes resulting from the high Doppler factor.

The parameters of the SSC model optimized for the broadband spectra are close to equipartition (kinetic energy density is $\approx 3 \times 10^{-5}$ erg cm^{-3}, magnetic energy density is $\approx 2 \times 10^{-5}$ erg cm^{-3}), although this was not a restriction for the model. The energy of the emitting electrons contained in the emission region of the jet, that is responsible for the broadband emission up to very high energies, is $E \approx 9 \times 10^{48}$ erg.

Despite the overall match, this one component synchrotron model is disfavoured by the variability characteristics, e.g. the variability time scale of some days, described in Sect. 3. In light of the inability of the one-zone SSC model to explain the variability, the use of such a model as a physical representation of the blazar jet should be considered an approximation.

Comparison of the high synchrotron state in this 2009 multi-wavelength campaign to earlier observations would require changes to the SSC model. Between 2004 and 2009 the X-ray flux changed by a factor of ~50 and the spectrum changed from a broken power law with photon indices of $\Gamma_1 = 3.1$ and $\Gamma_2 = 2.6$ and a break at 2.5 keV (H.E.S.S. Collaboration 2010) to a broken power law with photon indices $\Gamma_1 = 2.0$ and $\Gamma_2 = 2.5$ and with a break at 3.8 keV as can be seen in Fig. 4. During this time the TeV emission showed small variation in flux with no significant change in slope. No trivial change in parameters of the one zone SSC model used to represent the 2009 multi-wavelength spectra can describe the steep X-ray spectrum measured in 2004. The specific change in shape of the synchrotron emission peak can be sketched using indices of $n_1 = 2$ and $n_2 = 4.8$ for the broken power law of the electron distribution. But this would mean an arbitrary change of 2.8 of the photon indices lacking any physics basis. Multi-component models do not have this problem. However, given the wavelength coverage and the limited signal-to-noise in fine time-bins, multi-component models remain ambiguous.

As shown in H.E.S.S. Collaboration (2010), between 2004 and 2005, the X-ray flux increased by a factor of ~16 without significant increase of the TeV flux. With the large X-ray flux state detected in 2009, the difference in the X-ray flux to 2004 is much higher (factor of ~50) with still only marginal increase of the TeV flux by ~2.

5. Summary and conclusions

A broadband multi-wavelength campaign on PKS 2005-489 with, for the first time, simultaneous observations in the VHE γ-ray (by H.E.S.S.), HE γ-ray (*Fermi*/LAT), X-ray (RXTE, Swift), UV (Swift) and optical (ATOM, Swift) band has been conducted between May 22 and July 2, 2009. PKS 2005-489 was observed in a very bright X-ray state, comparable to the historical maximum. The optical flux at the beginning of the campaign was also the highest in several years. For the first time such a high state in synchrotron emission for PKS 2005-489 was covered by γ-ray observations with *Fermi*/LAT and H.E.S.S. Variability in the VHE γ-ray emission and a decrease in flux in the X-ray and optical bands were detected. Considering a longer time range of 22 months, variations could be detected in the HE γ-ray band with an amplitude similar to the variation of the optical emission.

The simultaneously measured hard HE spectrum connects well to the VHE spectrum resulting in a peak of the inverse Compton emission between ~5 and ~500 GeV. These characteristics are compatible with the long term behaviour in the γ-ray

band, while the inverse Compton peak is at higher energies during this campaign due to the higher VHE flux and the curved spectrum measured. The observed X-ray spectrum obtained during the campaign shows a clear break at ~4 keV indicating the cutoff of the synchrotron emission. The hard photon index up to the break energy is one of the main differences of previous X-ray observations in a lower flux state.

These multi-wavelength observations cover well the two emission peaks in the spectral energy distribution. A one zone SSC model was used to fit the broadband spectra. The characteristic broken power law shape of the X-ray spectrum yields a clear break of the synchrotron emission, restricting the parameter range of the SSC model.

In comparison with previous observations in the X-ray and TeV γ-ray range of 2004 (H.E.S.S. Collaboration 2010), the X-ray flux has changed by a factor of ~50 while the VHE γ-ray flux shows smaller variations by a factor of ~2. This large change in synchrotron emission with very small changes in inverse Compton emission is unusual for high-frequency peaked BL Lac objects. Especially the change in spectral shape in the X-ray range between 2004 and 2009 is not reflected in the inverse Compton range.

The prominent TeV blazars, Mrk 421 and PKS 2155-304, have been observed simultaneously in the X-ray and VHE band several times. An interesting aspect of study is the relation of the X-ray and VHE flux during different flaring states of these sources. For PKS 2155-304 a cubic relation ($F_\gamma \propto F_X^3$) was found during a flare in 2006 (Aharonian et al. 2009a), which means that the VHE flux showed a much stronger variation than the X-ray flux. For Mrk 421, a period with several flares occured in 2001, which was covered by observations of RXTE, Whipple and HEGRA (Fossati et al. 2008). The resulting relations of the X-ray and VHE flux changed from $\beta = 0.5$ to $\beta = 2$ ($F_\gamma \propto F_X^\beta$) (Fossati et al. 2008). The simultaneous X-ray and VHE measurement of PKS 2005-489 in 2004 and 2009 exhibit a different behaviour. The X-ray flux varies strongly while VHE fluxes hardly change which yield $\beta = 0.2$. Contrary to the other sources, this may imply that during the flare the electron population changes such that the IC scattering occurs predominantly in the Klein-Nishina regime, which has lower efficiency for production of TeV photons, while it is (largely) in the Thomson regime during quiescence.

The huge changes in synchrotron emission with small changes in inverse Compton emission over the years between low and high flux states in the synchrotron branch of PKS 2005-489 challenge the applicability of a one zone SSC model to this source. A similar conclusion about the limitations of a one-zone SSC model was reached for the multi-wavelength campaign on PKS 2155-304 (Aharonian et al. 2009b). Results such as these emphasize the need for sustained or repeated multi-wavelength campaigns to measure spectral variability.

References

Abdo, A. A., Ackermann, M., Ajello, M., et al. (Fermi-LAT Collaboration) 2010, ApJS, 188, 405

Abdo, A. A., Ackermann, M., Ajello, M., et al. (Fermi-LAT Collaboration) 2009, ApJ, 707, 1310

Aharonian, F., Akhperjanian, A. G., Anton, G., et al. (H.E.S.S. Collaboration) 2009a, A&A, 502, 749

Aharonian, F., Akhperjanian, A. G., Anton, G., et al. (H.E.S.S. Collaboration & Fermi-LAT Collaboration) 2009b, ApJ, 696, L150

Aharonian, F., Akhperjanian, A. G., Aye, K.-M., et al. (H.E.S.S. Collaboration) 2005, A&A, 436, L17

Aharonian, F., Akhperjanian, A. G., Aye, K.-M., et al. (H.E.S.S. Collaboration) 2004, Astrop. Phys., 22, 109

Aharonian, F., Akhperjanian, A. G., Bazer-Bachi, A. R., et al. (H.E.S.S. Collaboration) 2006a, A&A, 457, 899

Aharonian, F., Akhperjanian, A. G., Bazer-Bachi, A. R., et al. (H.E.S.S. Collaboration) 2006b, Nature, 440, 1018

Atwood, W. B., Abdo, A. A., Ackermann, M., et al. (Fermi-LAT Collaboration) 2009, ApJ, 697, 1071

Bessell, M. S. 1990, PASP, 102, 1181

Bradt, H. V., Rothschild, R. E., & Swank, J. H. 1993, A&AS, 97, 355

Burrows, D. N., Hill, J. E., Nousek, J. A., et al. 2005, Space Sci. Rev., 120, 165

Cash, W. 1979, ApJ, 228, 939

Cheung, C. C., Urry, C. M., Scarpa, R., & Giavalisco, M. 2003, ApJ, 599, 155

Falomo, R., Maraschi, L., Treves, A., & Tanzi, E. G. 1987, ApJ, 318, L39

Fossati, G., Buckley, J. H., Bond, I. H., et al. 2008, ApJ, 677, 906

Franceschini, A., Rodighiero, G., & Vaccari, M. 2008, A&A, 487, 837

Fukugita, M., Shimasaku, K., & Ichikawa, T. 1995, PASP, 107, 945

Giommi, P., Blustin, A. J., Capalbi, M., et al. 2006, A&A, 456, 911

Godet, O., Beardmore, A. P., Abbey, A. F., et al. 2009, A&A, 494, 775

Hauser, M., Möllenhoff, C., Pühlhofer, G., et al. 2004, Astron. Nachr., 325, 659

H.E.S.S. Collaboration. 2010, A&A, 511, 52

Johnston, K. J., Fey, A. L., Zacharias, N., et al. 1995, AJ, 110, 880

Kalberla, P. M. W., Burton, W. B., Hartmann, D., et al. 2005, A&A, 440, 775

Krawczynski, H., Hughes, S. B., Horan, D., et al. 2004, ApJ, 601, 151

Kühr, H., Witzel, A., Pauliny-Toth, I. I. K., & Nauber, U. 1981, A&AS, 45, 367

Li, T., & Ma, Y. 1983, ApJ, 272, 317

Lin, Y. C., Bertsch, D. L., Bloom, S. D., et al. 1999, ApJ, 525, 191

Mannheim, K. 1993, A&A, 269, 67

Marscher, A. P., & Gear, W. K. 1985, ApJ, 298, 114

Mattox, J. R., Bertsch, D. L., Chiang, J., et al. 1996, ApJ, 461, 396

Monet, D. et al. 1998, VizieR Online Data Catalog, 1252, 0

Moshir, M. 1990, in IRAS Faint Source Catalogue, version 2.0

Nandikotkur, G., Jahoda, K. M., Hartman, R. C., et al. 2007, ApJ, 657, 706

Perlman, E. S., Madejski, G., Stocke, J. T., & Rector, T. A. 1999, ApJ, 523, L11

Poole, T. S., Breeveld, A. A., Page, M. J., et al. 2008, MNRAS, 383, 627

Ricci, R., Prandoni, I., Gruppioni, C., Sault, R. J., & de Zotti, G. 2006, A&A, 445, 465

Roming, P. W. A., Kennedy, T. E., Mason, K. O., et al. 2005, Space Sci. Rev., 120, 95

Scarpa, R., Urry, C. M., Falomo, R., Pesce, J. E., & Treves, A. 2000, ApJ, 532, 740

Schlegel, D. J., Finkbeiner, D. P., & Davis, M. 1998, ApJ, 500, 525

Tagliaferri, G., Ghisellini, G., Giommi, P., et al. 2001, A&A, 368, 38

Tingay, S. J., Jauncey, D. L., King, E. A., et al. 2003, PASJ, 55, 351

Wall, J. V., Shimmins, A. J., & Bolton, J. G. 1975, Aust. J. Phys. Astrophys. Suppl., 34, 55

[1] Universität Hamburg, Institut für Experimentalphysik, Luruper Chaussee 149, 22761 Hamburg, Germany

[2] Laboratoire de Physique Théorique et Astroparticules, Université Montpellier 2, CNRS/IN2P3, CC 70, Place Eugène Bataillon, 34095 Montpellier Cedex 5, France

[3] Max-Planck-Institut für Kernphysik, PO Box 103980, 69029 Heidelberg, Germany

[4] Dublin Institute for Advanced Studies, 31 Fitzwilliam Place, Dublin 2, Ireland

[5] National Academy of Sciences of the Republic of Armenia, Yerevan, Armenia

[6] Yerevan Physics Institute, 2 Alikhanian Brothers St., 375036 Yerevan, Armenia

[7] Universität Erlangen-Nürnberg, Physikalisches Institut, Erwin-Rommel-Str. 1, 91058 Erlangen, Germany

[8] Nicolaus Copernicus Astronomical Center, ul. Bartycka 18, 00-716 Warsaw, Poland

[9] CEA Saclay, DSM/IRFU, 91191 Gif-Sur-Yvette Cedex, France

[10] University of Durham, Department of Physics, South Road, Durham DH1 3LE, UK

[11] Centre d'Étude Spatiale des Rayonnements, CNRS/UPS, 9 Av. du Colonel Roche, BP 4346, 31029 Toulouse Cedex 4, France

[12] Astroparticule et Cosmologie (APC), CNRS, Université Paris 7 Denis Diderot, 10, rue Alice Domon et Léonie Duquet, 75205 Paris Cedex 13 (UMR 7164: CNRS, Université Paris VII, CEA, Observatoire de Paris), France

[13] Laboratoire Leprince-Ringuet, École Polytechnique, CNRS/IN2P3, 91128 Palaiseau, France
e-mail: fortin@llr.in2p3.fr

[14] Institut für Theoretische Physik, Lehrstuhl IV: Weltraum und Astrophysik, Ruhr-Universität Bochum, 44780 Bochum, Germany

[15] Landessternwarte, Universität Heidelberg, Königstuhl, 69117 Heidelberg, Germany
e-mail: S.Kaufmann@lsw.uni-heidelberg.de

[16] Institut für Physik, Humboldt-Universität zu Berlin, Newtonstr. 15, 12489 Berlin, Germany

[17] LUTH, Observatoire de Paris, CNRS, Université Paris Diderot, 5 Place Jules Janssen, 92190 Meudon, France

[18] LPNHE, Université Pierre et Marie Curie Paris 6, Université Denis Diderot Paris 7, CNRS/IN2P3, 4 Place Jussieu, 75252, Paris Cedex 5, France

[19] Institut für Astronomie und Astrophysik, Universität Tübingen, Sand 1, 72076 Tübingen, Germany

[20] Astronomical Observatory, The University of Warsaw, Al. Ujazdowskie 4, 00-478 Warsaw, Poland

[21] Unit for Space Physics, North-West University, Potchefstroom 2520, South Africa

[22] Laboratoire d'Annecy-le-Vieux de Physique des Particules, Université de Savoie, CNRS/IN2P3, 74941 Annecy-le-Vieux, France

[23] Oskar Klein Centre, Department of Physics, Stockholm University, Albanova University Center, 10691 Stockholm, Sweden

[24] University of Namibia, Department of Physics, Private Bag 13301, Windhoek, Namibia

[25] Laboratoire d'Astrophysique de Grenoble, INSU/CNRS, Université Joseph Fourier, BP 53, 38041 Grenoble Cedex 9, France

[26] Instytut Fizyki Jądrowej PAN, ul. Radzikowskiego 152, 31-342 Kraków, Poland

[27] Institut für Astro- und Teilchenphysik, Leopold-Franzens-Universität Innsbruck, 6020 Innsbruck, Austria

[28] Department of Physics and Astronomy, The University of Leicester, University Road, Leicester, LE1 7RH, UK

[29] Obserwatorium Astronomiczne, Uniwersytet Jagielloński, ul. Orla 171, 30-244 Kraków, Poland

[30] Toruń Centre for Astronomy, Nicolaus Copernicus University, ul. Gagarina 11, 87-100 Toruń, Poland

[31] School of Chemistry & Physics, University of Adelaide, Adelaide 5005, Australia

[32] Charles University, Faculty of Mathematics and Physics, Institute of Particle and Nuclear Physics, V Holešovičkách 2, 180 00 Prague 8, Czech Republic

[33] European Associated Laboratory for Gamma-Ray Astronomy, jointly supported by CNRS and MPG, France

[34] Oskar Klein Centre, Department of Physics, Royal Institute of Technology (KTH), Albanova, 10691 Stockholm, Sweden

[35] School of Physics & Astronomy, University of Leeds, Leeds LS2 9JT, UK

[36] National Research Council Research Associate, National Academy of Sciences, Washington, DC 20001, resident at Naval Research Laboratory, Washington, DC 20375, USA

[37] W. W. Hansen Experimental Physics Laboratory, Kavli Institute for Particle Astrophysics and Cosmology, Department of Physics and SLAC National Accelerator Laboratory, Stanford University, Stanford, CA 94305, USA

[38] Istituto Nazionale di Fisica Nucleare, Sezione di Pisa, 56127 Pisa, Italy

[39] Istituto Nazionale di Fisica Nucleare, Sezione di Trieste, 34127 Trieste, Italy

[40] Dipartimento di Fisica, Università di Trieste, 34127 Trieste, Italy

[41] Istituto Nazionale di Fisica Nucleare, Sezione di Padova, 35131 Padova, Italy

[42] Dipartimento di Fisica "G. Galilei", Università di Padova, 35131 Padova, Italy

[43] Istituto Nazionale di Fisica Nucleare, Sezione di Perugia, 06123 Perugia, Italy

[44] Dipartimento di Fisica, Università degli Studi di Perugia, 06123 Perugia, Italy

[45] Dipartimento di Fisica "M. Merlin" dell'Università e del Politecnico di Bari, 70126 Bari, Italy

[46] Istituto Nazionale di Fisica Nucleare, Sezione di Bari, 70126 Bari, Italy

[47] Institut de Ciencies de l'Espai (IEEC-CSIC), Campus UAB, 08193 Barcelona, Spain

[48] NASA Goddard Space Flight Center, Greenbelt, MD 20771, USA
e-mail: `wmcconvi@umd.edu`

[49] University College Dublin, Belfield, Dublin 4, Ireland

[50] INAF-Istituto di Astrofisica Spaziale e Fisica Cosmica, 20133 Milano, Italy

[51] Agenzia Spaziale Italiana (ASI) Science Data Center, 00044 Frascati (Roma), Italy

[52] Center for Research and Exploration in Space Science and Technology (CRESST) and NASA Goddard Space Flight Center, Greenbelt, MD 20771, USA

[53] Department of Physics and Center for Space Sciences and Technology, University of Maryland Baltimore County, Baltimore, MD 21250, USA

[54] Space Science Division, Naval Research Laboratory, Washington, DC 20375, USA

[55] Department of Computational and Data Sciences, George Mason University, Fairfax, VA 22030, USA

[56] Université Bordeaux 1, CNRS/IN2p3, Centre d'Études Nucléaires de Bordeaux Gradignan, 33175 Gradignan, France

[57] CNRS/IN2P3, Centre d'Études Nucléaires Bordeaux Gradignan, UMR 5797, Gradignan, 33175, France

[58] Dipartimento di Fisica, Università di Udine and Istituto Nazionale di Fisica Nucleare, Sezione di Trieste, Gruppo Collegato di Udine, 33100 Udine, Italy

[59] Osservatorio Astronomico di Trieste, Istituto Nazionale di Astrofisica, 34143 Trieste, Italy

[60] Department of Physical Sciences, Hiroshima University, Higashi-Hiroshima, Hiroshima 739-8526, Japan

[61] INAF Istituto di Radioastronomia, 40129 Bologna, Italy

[62] Center for Space Plasma and Aeronomic Research (CSPAR), University of Alabama in Huntsville, Huntsville, AL 35899, USA

[63] Department of Physics, Center for Cosmology and Astro-Particle Physics, The Ohio State University, Columbus, OH 43210, USA

[64] Science Institute, University of Iceland, IS-107 Reykjavik, Iceland

[65] Research Institute for Science and Engineering, Waseda University, 3-4-1, Okubo, Shinjuku, 169-8555 Tokyo, Japan

[66] Centre d'Étude Spatiale des Rayonnements, CNRS/UPS, BP 44346, 30128 Toulouse Cedex 4, France

[67] Department of Physics and Department of Astronomy, University of Maryland, College Park, MD 20742, USA

[68] Istituto Nazionale di Fisica Nucleare, Sezione di Roma "Tor Vergata", 00133 Roma, Italy

[69] Department of Physics and Astronomy, University of Denver, Denver, CO 80208, USA

[70] Hiroshima Astrophysical Science Center, Hiroshima University, Higashi-Hiroshima, 739-8526 Hiroshima, Japan

[71] Institute of Space and Astronautical Science, JAXA, 3-1-1 Yoshinodai, Chuo-ku, Sagamihara, 252-5210 Kanagawa, Japan

[72] Max-Planck Institut für extraterrestrische Physik, 85748 Garching, Germany

[73] College of Science, George Mason University, Fairfax, VA 22030, resident at Naval Research Laboratory, Washington, DC 20375, USA

[74] Santa Cruz Institute for Particle Physics, Department of Physics and Department of Astronomy and Astrophysics, University of California at Santa Cruz, Santa Cruz, CA 95064, USA

[75] NYCB Real-Time Computing Inc., Lattingtown, NY 11560-1025, USA

[76] Department of Chemistry and Physics, Purdue University Calumet, Hammond, IN 46323-2094, USA

[77] Partially supported by the International Doctorate on Astroparticle Physics (IDAPP) program

[78] Institució Catalana de Recerca i Estudis Avançats (ICREA), Barcelona, Spain

[79] Consorzio Interuniversitario per la Fisica Spaziale (CIFS), 10133 Torino, Italy

[80] INTEGRAL Science Data Centre, 1290 Versoix, Switzerland

[81] NASA Postdoctoral Program Fellow, USA

[82] Dipartimento di Fisica, Università di Roma "Tor Vergata", 00133 Roma, Italy

[83] Department of Physics, Royal Institute of Technology (KTH), AlbaNova, 106 91 Stockholm, Sweden

[84] School of Pure and Applied Natural Sciences, University of Kalmar, 391 82 Kalmar, Sweden